

## Wear Behavior of Ti-xNb Biomedical Alloys by Ball Cratering

Felype N. de Mattos<sup>a</sup> , Pedro A. B. Kuroda<sup>b</sup>, Mariana C. Rossi<sup>b</sup>, Conrado R. M. Afonso<sup>b</sup> 

<sup>a</sup>Universidade Federal de São Carlos (UFSCar), 13565-905, São Carlos, SP, Brasil.

<sup>b</sup>Universidade Federal de São Carlos (UFSCar), Departamento de Engenharia de Materiais (DEMa), 13565-905, São Carlos, SP, Brasil.

Received: November 13, 2023; Accepted: December 21, 2023

Ti alloys have been developing through the years, aiming the biomedical application since it has suitable properties. Among Ti alloys, the Ti-Nb systems are a pronounced group to biomedical applications due to its low elastic modulus, good corrosion resistance, and mechanical properties. Although this system is quite well-known regarding its phases, structure and properties, there is not plenty of information about wear available in the literature. To investigate the wear resistance, the samples were submitted to x-ray diffraction (XRD) and scanning electron microscopy (SEM) to analyze the phases formed. Hardness and elastic modulus were measured by microhardness Vickers and dynamic Young modulus by excitation impulse. Additionally, wear volume, wear resistance, and H/E ratio were calculated to understand the wear material's performance. This study aims to investigate the wear resistance of Ti-xNb ( $x = 15, 25$  and  $40\text{wt.}\%$ ), one of each type of Ti alloys and phases formed: Ti-15Nb ( $\alpha'$ ), Ti-25Nb ( $\alpha''$ ) and Ti-40Nb ( $\beta$ ) and the influence of cooling rate after solution heat treatment on wear properties through ball cratering. It was possible to find that the harder the alloy, the higher the wear resistance. Thus, in the case of Ti-xNb ( $x = 15, 25$  and  $40\text{wt.}\%$ ), alloys the hardness plays a significant role in wear resistance. Besides that, the samples that have presented the  $\alpha'$  or  $\alpha''$  phase have the lowest wear resistance. Therefore, not only the hardness influences the wear resistance but also the combination of phases formed.

**Keywords:** *Ti alloys, low elastic modulus, wear resistance, micro abrasive ball cratering, structural characterization.*

### 1. Introduction

Ti and its alloys have been acclaimed for biomedical applications since they present suitable properties such as good corrosion resistance, excellent biocompatibility, and low elastic modulus<sup>1-3</sup>. Low elastic modulus is an expected and essential characteristic because of the mismatch of this property inducing the implant to stress shielding in the bone, which can lead to bone resorption and implant loosening (stress shielding)<sup>4,5</sup>. Therefore, alloys with elastic modulus nearer the human bone's elastic modulus are desirable. Among some possibilities of Ti alloys,  $\beta$  Ti alloys have been developed to produce a suitable alloy with an elastic modulus nearer the bone's modulus, thus increasing the implant service life. For instance, Ti-25Ta-Zr-Nb, Ti-35Nb-7Zr-5Ta, Ti-15Zr-10Mo and Ti-Nb systems<sup>5,6</sup>, with good biocompatibility and low elastic modulus (50-80 GPa) have been developed for biomedical application. Ti-Nb system presents low elastic modulus, which can be explained by the presence of  $\beta$  phase in some alloys.  $\beta$  phase presents a less dense packing of atoms in its body-centered cubic (bcc) structure in comparison with  $\alpha$  phase, hexagonal close-packed (hcp). Yet, the presence of  $\alpha'$  and  $\alpha''$  also have been associated to the decreasing of elastic modulus<sup>7-9</sup>. In addition, Nb is an excellent  $\beta$  phase stabilizer, plays a significant role in reducing the elastic modulus improving Ti-based alloys'

corrosion resistance<sup>10,11</sup>. Besides that, it is essential to say that Nb has a relatively lower melting temperature than other  $\beta$  phase stabilizers, such as V, Ta, and Mo, resulting in less energy consumption. Furthermore, it was shown through invitro and vivo tests that adding Nb may improve bone tissue adhesion and proliferation.

Several studies devoted to Ti-Nb system has been published in recent past years. These studies proposed to investigate different aspects of this system, such as characterizing the structure and phase composition<sup>12</sup>, lattice parameters<sup>13</sup>, mechanical properties<sup>14</sup> and, biocompatibility. Although a considerable number of studies have been conducted to understand the relations between structure and properties, only a few studies devoted themselves to investigating the wear behavior of the Ti-Nb system. Wear behavior is an essential material property since it plays an important role in the time life of the material, which is crucial in biomedical applications.

The wear mechanism identified in orthopedic implant can be abrasive and might be related with material composition, hardness and surface properties<sup>15</sup> Ureña et al.<sup>16</sup> studied surface modification and showed that Ti-Nb coating improve wear behavior of Titanium. Alberta et al.<sup>17</sup> studied tribocorrosion of a  $\beta$ - Ti alloy (Ti-Nb-Ga), they showed Ga addition increase wear resistance of Ti-45Nb. Besides that, authors have reported a better understanding about tribocorrosion

\*e-mail: [felype.mattos@ifsudestemg.edu.br](mailto:felype.mattos@ifsudestemg.edu.br)

mechanism in a simple simulated body fluid. Asl et al.<sup>18</sup> showed that an anodized coating may improve wear behavior of Ti-Nb alloys. Gonçalves et al.<sup>19</sup> showed that tribocorrosion properties can be improved when a  $\beta$ -Ti alloy is reinforced with NbC addition.

This study aims to analyze the wear behavior through micro-ball cratering of Ti-xNb ( $x = 15, 25$  and  $40\text{wt}\%$ ) and compare this processing with two different heat treatments conditions regarding cooling rate (slowly and rapid cooled) imposed from the solid state. The characterization was conducted by the XRD patterns, followed by SEM analysis, hardness, elastic modulus tests, and wear resistance. In the end, it is shown, even in the as-cast state, it is possible to obtain an alloy with an elastic modulus as low as 53 GPa and good wear behavior.

## 2. Experimental Procedure

The ingots of Ti-xNb ( $x = 15, 25$  and  $40\text{wt}\%$ ) were obtained by copper mold suction casting in a compact arc melting furnace, Edmund-Bühler MAM-1, under an inert atmosphere with argon. These samples were named CM (copper mold). Besides that, some samples of these alloys were submitted to different heat treatment when it comes to cooling rate, rapid cooling (RC) upon water quenching and slow cooling (SC) under furnace cooling. Both treatments had a heating rate of  $10\text{ }^\circ\text{C}/\text{min}$  and treatment temperature of  $1000\text{ }^\circ\text{C}$  but one was cooled in furnace (SC) and the other in water (RC). It was used an suction cast arc melting furnace EDG under vacuum atmosphere with  $10^{-7}$  torr. After suction cast and heat treatment the samples were submitted to XRD, Bruker D8 Advanced-ECO Diffractometry, to analyses the phases formed. In addition, the hardness was measured by Shimadzu microhardness HMV G2 while to measure the elastic modulus dynamic young's modulus through ATCP Sonelastic equipment were used. For the hardness test the ASTM E384 was used and ASTM E1876 was adopted for the elastic modulus measurement. Finally, Optical Microscopy (OM), scanning electron microscopy (SEM) equipped with an energy dispersive X-ray detector (EDS) Phillips XL30 were used to observe the microstructure and homogeneity of the alloying elements. For the wear tests under dry system, it was used steel balls (AISI 52100, diameter of 25.4 mm and hardness 818 HV) rotating at 200 revolutions per minute (rpm) along 60 min, producing wear craters. For such tests, a 200 g load was used. The wear volume ( $V$ ) in  $\mu\text{m}^3$  and wear coefficient ( $K$ ) are calculated derived from Archard's law. For such analysis, measurement through image analysis (ImageJ) is done on the inner diameter of the crater.

## 3. Results and Discussion

Table 1 depicts the chemical composition through EDS analysis of all alloys in CM condition. It has shown that the

melting process was satisfactory, once Ti and Nb elements are in the expected concentration. In the production of titanium alloys, there is an ASTM standard for the commercial Ti-15Mo alloy, which stipulates that an experimental alloy with 14 and 16% Mo by weight can be classified as Ti-15Mo, that is, in the production of a binary alloy containing molybdenum an error of approximately 1% is acceptable. In light of the norm and performing a slight extrapolation for the Ti-Nb alloys, it is observed that all the alloys developed in this work are within the error stipulated by the norm, where the amount of experimental niobium is less than 1%, indicating that all mergers were carried out satisfactorily<sup>20</sup>.

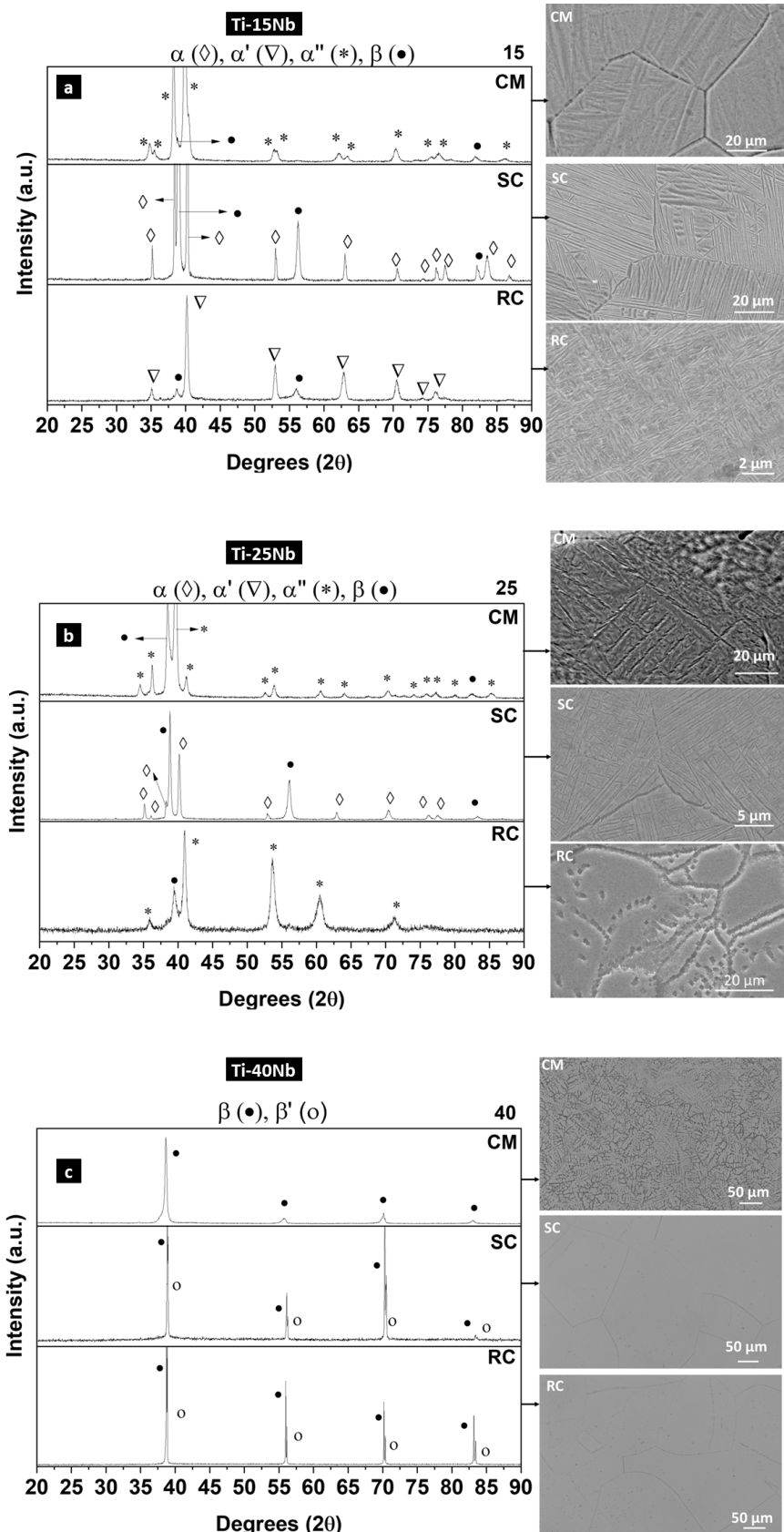
The XRD patterns and SEM images corresponding to all alloys and conditions are shown in Figure 1. Regarding Ti-15Nb, CM sample presents an almost completely  $\alpha''$  structure, while SC is showing a structure nearer to equilibrium condition  $\alpha + \beta$ , which is expected since the imposed cooling condition, and RC presents  $\alpha'$  and  $\beta$  phases. It was possible to see that heat treatment induces alloys to different phases, so it plays a significant role in phase transformation and in the XRD patterns. Besides that, it was observed that SC could separate the phases clearly and form finer peaks compared to sample RC and the one without heat treatment.

Regarding Ti-25Nb, it was noticed similar behavior to 15 Nb. The RC sample was induced to  $\alpha'' + \beta$  phase whereas SC was induced to  $\alpha + \beta$  and CM was induced to  $\alpha'' + \beta$  phases. Nevertheless, the SC sample has presented finer and clearer peaks than others. Finally, in the XRD pattern of 40Nb, only bcc structure was present in all conditions. The MC sample has presented only the  $\beta$  phase, whereas the SC and RC have presented not only the  $\beta$  phase but also a  $\beta'$  phase. The high content of the  $\beta$ -stabilizer element may explain it; when there is a high quantity of a  $\beta$ -stabilizer solute, it is possible to form a new  $\beta$  phase, which is called  $\beta'$ , with different lattice parameter and chemical composition through spinodal decomposition. These results are in agreement with literature<sup>21,22</sup>.

The microstructure of all Nb content and alloy conditions are also shown in Figure 1, and it can confirm the XRD patterns. Firstly, it is possible to observe some needles and grains 15 CM, only needles due to rapid cooling in 15 RC and grains and a lamellar structure in 15 SC, which is expected since the cooling is nearer equilibrium. Secondly, in the 25 CM is noticed some  $\alpha''$  needles and  $\beta$  grains, while in RC condition was possible to notice more grains than in 25 MC and some tiny needles; In the SC condition, it was found that the  $\alpha$  and  $\beta$  structures, very similar to the 15 SC conditions (due to the conditions nearer equilibrium). Finally, the 40 RC and SC showed a similar granular structure due to the  $\beta$ -stabilizer element content. Differently from them, 40 MC has presented an utterly dendritic structure, which is common in processing with mold. The results found here are in coherence with the ones found in the literature<sup>21,23-25</sup>.

**Table 1.** Semi-quantitative chemical composition from EDS analysis of all Ti-xNb alloys (weight%).

	Ti-15Nb	Ti-25Nb	Ti-40Nb
Ti (wt.%)	85 ± 1	77 ± 1	60 ± 1
Nb (wt.%)	15 ± 1	23 ± 2	40 ± 1



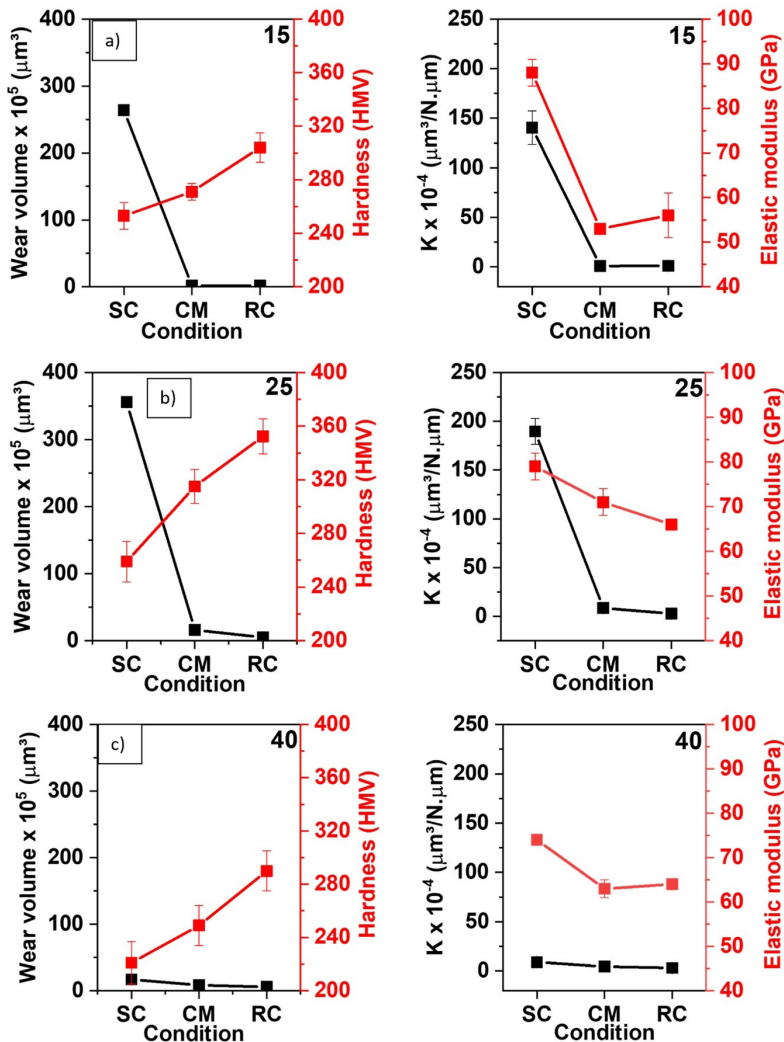
**Figure 1.** XRD patterns and SEM micrographs of (a) Ti-15Nb (b) Ti-25Nb and (c) Ti-40Nb in three different conditions: CM (copper mold), SC (slowly cooled), RC (rapidly cooled).

Figure 2 shows the variation of hardness, elastic modulus, wear coefficient and volume according to Nb content and sample condition. In Figure 2a is presented the results of Ti-15Nb and it is noticed that wear volume varies according to hardness in a clear tendency. The lower hardness the higher wear volume. The established phases in condition SC were  $\alpha + \beta$  and the decrease of hardness is related with  $\alpha$  phase as showed by Lee et al<sup>8</sup>. Therefore, the found results points to an increase of wear volume when  $\alpha$  phase is established. When it comes to wear coefficient (K) the tendency is different. The higher elastic modulus, the higher K and the highest K is presented by SC condition. In both cases, wear volume and coefficient, the results presented by CM and RC conditions did not vary significantly since it has similar hardness and elastic modulus although it has presented different phases. The hardness and elastic modulus results are in accordance with literature<sup>21-25</sup>

In Figure 2b it is presented the results of Ti-25Nb. It was observed a similar result that 15Nb and the wear volume varies according to hardness. Besides that, the highest wear

volume value is found in the samples with the lowest hardness value. It is also related with the  $\alpha$  phase established in this samples since the SC condition leads to the presence of this phase. The hardness value is in accordance with literature. Otherwise, the elastic modulus showed by CM and RC showed a lower value than the related in literature. It might be explained by the suppression of  $\omega$  phase, which increase the elastic modulus of Ti alloys and the phase was not found in XRD patterns<sup>26,27</sup>. Yet, the highest elastic modulus the highest K as found as in Ti-15Nb.

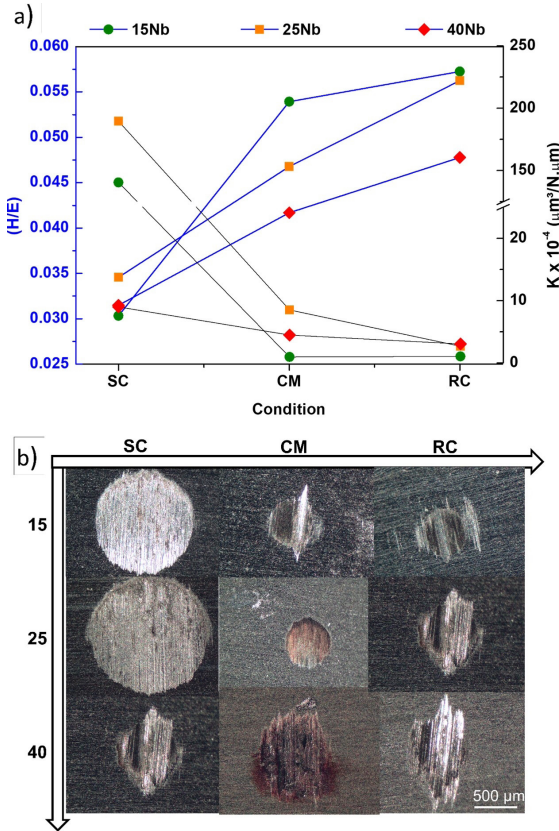
In Figure 2c is presented the results of Ti-40Nb. It was observed the same tendency that it was observed in 15 and 25 Nb and the found results are in accordance with literature<sup>28</sup>. However, it may be explained by other mechanism since the 40Nb did not present  $\alpha$  phase. The heat treatment is able to explain these differences since cooling rate plays a significant role in materials properties. SC condition might establish a big gran size while RC establish a smaller one<sup>29</sup>. Besides that, the internal stress can change the mechanical properties and tends to be higher in RC than SC<sup>30</sup>.



**Figure 2.** Wear volume x Vicker microhardness and Wear coefficient x Elastic modulus of Ti-15Nb (a), Ti-25Nb (b) and Ti-40Nb (c) in three different conditions: CM (copper mold), SC (slowly cooled), RC (rapidly cooled).

**Table 2.** Wear coefficient (K) and H/E ratio results of Ti-xNb alloys in all conditions.

	Ti-15Nb		Ti-25Nb		Ti-40Nb	
	K ( $\mu\text{m}^3/\text{N}\cdot\mu\text{m}$ )	H/E	K ( $\mu\text{m}^3/\text{N}\cdot\mu\text{m}$ )	H/E	K ( $\mu\text{m}^3/\text{N}\cdot\mu\text{m}$ )	H/E
SC	1.0E-2	0.03	2.0E-2	0.03	9.0E-4	0.03
CM	9.6E-5	0.05	8.5E-4	0.05	4.5E-4	0.04
RC	1.1E-4	0.06	2.7E-4	0.06	3.0E-4	0.05

**Figure 3.** H/E ratio x Wear coefficient of Ti-15Nb, Ti-25Nb, Ti-40Nb and its marks caused by ball cratering in three different conditions: CM (copper mold), SC (slowly cooled), RC (rapidly cooled).

Regarding the wear volume the authors observed a clear relation between wear behavior and hardness as presented in Figure 2 and there is no significant difference between CM and RC in all conditions. CM and RC lead the alloys to similar hardness and because of that the route processing did not affect the wear behavior since they are inducing to  $\alpha'$  or  $\alpha''$  phases. On the other hand, the SC condition induced a pronounced difference on wear volume of the samples. SC condition presented the lowest value of hardness and in these samples were found the highest wear volume values, which suggest the combination of  $\alpha + \beta$ , principally  $\alpha$  presence, are easier to be worn than others. Different from the others, 40 Nb has presented a different rule. Since it is completely  $\beta$  structure there is no huge difference between the samples independent of the condition, although this fact the tendency presented is the same that one found in 15 and 25 Nb.

Besides, was noticed that Nb content reduce the wear volume, which was also related in literature<sup>31,32</sup>.

There is a correlation between wear behavior and mechanical properties know as H/E ratio (Hardness/ Elastic modulus) and the classical theories of wear points to hardness as a key parameter in wear controlling<sup>33,34</sup>. The harder material the best wear resistance and it is related that if  $H/E > 0.04$  the alloy exhibits a good wear resistance<sup>24,25</sup>. H/E was calculated in this study and is shown in Figure 3. It is clear that there is a clear tendency and the authors observed that H/E is inverse to wear coefficient. The worst result of H/E is presented by SC condition, which is smaller than 0.04 and it is in accordance with literature since the SC sample induce the lowest hardness value. Therefore, the SC condition is not convenient to be applied when high wear resistance is required. The CM and RC condition are similar and both of them presented satisfactory results of H/E, being RC lightly higher than CM. Additionally, the results of K and H/E are also presented in Table 2.

#### 4. Conclusions

The CM process was enough to ensure chemical homogeneity to all Nb content alloys. It was noticed that CM condition led to  $\alpha''$  martensite, RC lead to  $\alpha'$  martensite phase for 15Nb alloy and SC lead to  $\alpha + \beta$  phases. In 25Nb alloy the  $\alpha''$  martensite is formed in CM and RC conditions, whereas SC establish  $\alpha + \beta$  phases closer to equilibrium condition. The 40Nb formed  $\beta$  phase in all conditions (SC and CM) and when submitted to heat treatment followed by and RC lead to the formation of  $\beta + \beta'$  phase separation. Hardness and elastic modulus are associated with phases formed for each alloy. It is confirmed that  $\alpha + \beta$  structure in 15Nb and 25Nb alloys lead to the lowest hardness and highest elastic modulus due to  $\alpha$  phase fraction. The CM and RC conditions presented similar values for mechanical properties in 15 and 25Nb alloys. The 40Nb alloy has presented similar results in CM and RC samples and also presented the lowest hardness and highest elastic modulus in SC condition as 15 and 25Nb alloys. However, it is associated with greater grain size since 40Nb alloy has presented only  $\beta$  or  $\beta + \beta'$  phase. Regarding wear behavior, it was possible to conclude that it follows an inverse tendency to wear coefficient and hardness. CM and RC samples did not present a significant difference regarding H/E ratio since it presents similar phases and hardness values. The lowest hardness values are associated with  $\alpha$  phase in 15% and 25%Nb alloys and with a greater  $\beta$  grain size in 40%Nb alloy. Therefore, the greater the  $\alpha$  phase fraction and the higher the grain size lead to a decreasing in the wear resistance of the alloys.

## 5. Acknowledgments

This study was financed partly by the Coordenação de Aperfeiçoamento de Pessoal de Nível Superior of Brazil (CAPES), Finance Code 001. The authors would like to thank the “IF Sudeste MG - Campus Juiz de Fora”. The authors wish to thank the Brazilian agencies: the CNPq Universal Project #422015/2018-0 (C.R.M.A.) and the FAPESP (São Paulo Research Foundation) for financial support through “Projeto Temático” #2018/18293-8 and FAPESP post-doc grants #2019/26517-6 (P.A.B.K.), #2021/03865-9 (M.C.R) whom the authors thank.

## 6. References

- Afonso CRM, Amigó A, Stolyarov V, Gunderov D, Amigó V. From porous to dense nanostructured  $\beta$ -Ti alloys through high-pressure torsion. *Sci Rep.* 2017;7(1):13618. <http://dx.doi.org/10.1038/s41598-017-13074-z>.
- Schmidt R, Pilz S, Lindemann I, Damm C, Hufenbach J, Helth A, et al. Powder metallurgical processing of low modulus  $\beta$ -type Ti-45Nb to bulk and macro-porous compacts. *Powder Technol.* 2017;322:393-401. <http://dx.doi.org/10.1016/j.powtec.2017.09.015>.
- Pandey AK, Gautam RK, Behera CK. Corrosion and wear behavior of Ti-5Cu-xNb biomedical alloy in simulated body fluid for dental implant applications. *J Mech Behav Biomed Mater.* 2023;137:105533. <http://dx.doi.org/10.1016/j.jmbbm.2022.105533>.
- Cardoso GC, Buzalaf MAR, Correa DRN, Grandini CR. Effect of thermomechanical treatments on microstructure, phase composition, vickers microhardness, and Young's modulus of Ti-xNb-5Mo alloys for biomedical applications. *Metals.* 2022;12(5):788. <http://dx.doi.org/10.3390/met12050788>.
- Kuroda PAB, Quadros FF, Araujo RO, Afonso CRM, Grandini CR. Effect of thermomechanical treatments on the phases, microstructure, microhardness and Young's modulus of Ti-25Ta-Zr alloys. *Materials.* 2019;12(19):3210. <http://dx.doi.org/10.3390/ma12193210>.
- Kuroda PAB, Grandini CR, Afonso CRM. Surface characterization of new  $\beta$  Ti-25Ta-Zr-Nb alloys modified by micro-arc oxidation. *Materials.* 2023;16(6):2352. <http://dx.doi.org/10.3390/ma16062352>.
- Pérez DAG, Jorge AM Jr, Roche V, Lepretre J-C, Afonso CRM, Travessa DN, et al. Severe plastic deformation and different surface treatments on the biocompatible Ti13Nb13Zr and Ti35Nb7Zr5Ta alloys: microstructural and phase evolutions, mechanical properties, and bioactivity analysis. *J Alloys Compd.* 2020;812:152116. <http://dx.doi.org/10.1016/j.jallcom.2019.152116>.
- Lee CM, Ju CP, Lin JHC. Structure - property relationship of cast Ti-Nb alloys. *J Oral Rehabil.* 2002;29(4):314-22. <http://dx.doi.org/10.1046/j.1365-2842.2002.00825.x>.
- Gonzalez ED, Afonso CRM, Nascente PAP. Influence of Nb content on the structure, morphology, nanostructure, and properties of Titanium-Niobium Magnetron sputter deposited coatings for biomedical applications. *Surf Coat Tech.* 2017;326:424. <http://dx.doi.org/10.1016/j.surfcoat.2017.03.015>.
- Santos RFM, Ricci VP, Afonso CRM. Continuous cooling transformation (CCT) diagrams of  $\beta$  Ti-40Nb and TMZF alloys and influence of cooling rate on microstructure and elastic modulus. *Thermochim Acta.* 2022;717:179341. <http://dx.doi.org/10.1016/j.tca.2022.179341>.
- Santos RFM, Ricci VP, Afonso CRM. Influence of swaging on microstructure, elastic modulus and vickers microhardness of  $\beta$  Ti-40Nb Alloy for implants. *J Mater Eng Perform.* 2021;30(5):3363-9. <http://dx.doi.org/10.1007/s11665-021-05706-3>.
- Hon Y, Wang J, Pan Y. Composition/phase structure and properties of titanium-niobium alloys. *Mater Trans.* 2003;44(11):2384-90. <http://dx.doi.org/10.2320/matertrans.44.2384>.
- Thoemmes A, Bataev IA, Lazurenko DV, Ruktuev AA, Ivanov IV, Afonso CRM, et al. Microstructure and lattice parameters of suction-cast Ti-Nb alloys in a wide range of Nb concentrations. *Mater Sci Eng A.* 2021;818:141378. <http://dx.doi.org/10.1016/j.msea.2021.141378>.
- Kuroda PAB, da Silva LM, Sousa KSJ, Donato TAG, Grandini CR. Preparation, structural, microstructural, mechanical, and cytotoxic characterization of Ti-15Nb alloy for biomedical applications. *Artif Organs.* 2020;44(8):811-7. <http://dx.doi.org/10.1111/aor.13624>.
- Revathi A, Magesh S, Balla VK, Das M, Manivasagam G. Current advances in enhancement of wear and corrosion resistance of titanium alloys: a review. *Mater Technol.* 2016;31(12):696-704. <http://dx.doi.org/10.1080/10667857.2016.1212780>.
- Ureña J, Tabares E, Tsipas S, Jiménez-morales A, Gordo E. Dry sliding wear behaviour of  $\beta$ -type Ti-Nb and Ti-Mo surfaces designed by diffusion treatments for biomedical applications. *J Mech Behav Biomed Mater.* 2019;91:335-44. <http://dx.doi.org/10.1016/j.jmbbm.2018.12.029>.
- Alberta LA, Vishnu J, Douest Y, Perrin K, Trunfio-Sfarghiu A-M, Courtois N, et al. Tribocorrosion behavior of  $\beta$ -type Ti-Nb-Ga alloys in a physiological solution. *Tribol Int.* 2023;181:108325. <http://dx.doi.org/10.1016/j.triboint.2023.108325>.
- Asl HG, Sert Y, Küçükömeroğlu T, Bayrak O. The comparison of wear performances of CP-Ti, Ti6Al4V, Ti45Nb alloys oxidized by anodic oxidation under ambient air and vacuum conditions. *Mater Today Commun.* 2023;34:105466. <http://dx.doi.org/10.1016/j.mtcomm.2023.105466>.
- Gonçalves VRM, Corrêa DRN, Grandini CR, Pintão CAF, Afonso CRM, Lisboa PN Fo. Assessment of improved tribocorrosion in novel in-situ Ti and  $\beta$  Ti - 40Nb alloy matrix composites produced with NbC addition during arc-melting for biomedical applications. *Mater Chem Phys.* 2023;301:127597. <http://dx.doi.org/10.1016/j.matchemphys.2023.127597>.
- ASTM: American Society for Testing and Materials. ASTM F2066-18: standard specification for wrought Titanium-15 molybdenum alloy for surgical implant applications (UNS R58150). West Conshohocken: ASTM; 2017.
- Santos RF, Rossi MC, Vidilli AL, Amigó Borrás V, Afonso CRM. Assessment of  $\beta$  stabilizers additions on microstructure and properties of as-cast  $\beta$  Ti-Nb based alloys. *J Mater Res Technol.* 2023;22:3511-24. <http://dx.doi.org/10.1016/j.jmrt.2022.12.144>.
- Gonçalves VRM, Corrêa DRN, Grandini CR, Pintão CAF, Afonso CRM, Lisboa PN Fo. Assessment of improved tribocorrosion in novel in-situ Ti and  $\beta$  Ti-40Nb alloy matrix composites produced with NbC addition during arc-melting for biomedical applications. *Mater Chem Phys.* 2023;301:127597. <http://dx.doi.org/10.1016/j.matchemphys.2023.127597>.
- Çaha I, Alves AC, Chirico C, Maria Pinto A, Tsipas S, Gordo E, et al. Atomic-scale investigations of passive film formation on Ti-Nb alloys. *Appl Surf Sci.* 2023;615:156282. <http://dx.doi.org/10.1016/j.apsusc.2022.156282>.
- Wang H, Lai DKZ, Song C, Zhao Y, Cheng J, Bönisch M, et al. Zero thermal expansion and high Young's modulus in Ti-Nb achieved by concurrent  $\alpha'$ 's and  $\omega$  precipitation. *Scr Mater.* 2023;232:115477. <http://dx.doi.org/10.1016/j.scriptamat.2023.115477>.
- Fellah M, Hezil N, Touhami MZ, Obrosova A, Weiß S, Kashkarov EB, et al. Enhanced structural and tribological performance of nanostructured Ti-15Nb alloy for biomedical applications. *Results Phys.* 2019;15:102767. <http://dx.doi.org/10.1016/j.rinp.2019.102767>.
- Hsu HC, Wu SC, Hsu SK, Syu JY, Ho WF. The structure and mechanical properties of as-cast Ti-25Nb-xSn alloys for biomedical applications. *Mater Sci Eng A.* 2013;568:1-7. <http://dx.doi.org/10.1016/j.msea.2013.01.002>.

27. Kim SP, Kaseem M, Choe HC. Plasma electrolytic oxidation of Ti-25Nb-xTa alloys in solution containing Ca and P ions. *Surf Coat Tech.* 2020;395:125916. <http://dx.doi.org/10.1016/j.surfcoat.2020.125916>.
28. Hussein MA, Azeem MA, Kumar AM, Saravanan S, Ankah N, Sorour AA. Design and processing of near- $\beta$  Ti e Nb e Ag alloy with low elastic modulus and enhanced corrosion resistance for orthopedic implants. *J Mater Res Technol.* 2023;24:259-73. <http://dx.doi.org/10.1016/j.jmrt.2023.03.003>.
29. Lu JW, Zhao YQ, Ge P, Niu HZ. Microstructure and beta grain growth behavior of Ti-Mo alloys solution treated. *Mater Charact.* 2013;84(96):105-11. <http://dx.doi.org/10.1016/j.matchar.2013.07.014>.
30. Hildyard EM, Connor LD, Church NL, Whitfield TE, Martin N, Rugg D, et al. On the role of internal stresses on the superelastic behaviour of Ti-24Nb (at.%). *Acta Mater.* 2022;237:118161. <http://dx.doi.org/10.1016/j.actamat.2022.118161>.
31. Li SJ, Yang R, Li S, Hao YL, Cui YY, Niinomi M, et al. Wear characteristics of Ti-Nb-Ta-Zr and Ti-6Al-4V alloys for biomedical applications. *Wear.* 2004;257(9-10):869-76. <http://dx.doi.org/10.1016/j.wear.2004.04.001>.
32. Qiu J, Fu Z, Liu B, Liu Y, Yan J, Pan D, et al. Effects of niobium particles on the wear behavior of powder metallurgical  $\gamma$ -TiAl alloy in different environments. *Wear.* 2019;434-435:202964. <http://dx.doi.org/10.1016/j.wear.2019.202964>.
33. Leyland A, Matthews A. On the significance of the H/E ratio in wear control: a nanocomposite coating approach to optimised tribological behaviour. *Wear.* 2000;246(1-2):1-11. [http://dx.doi.org/10.1016/S0043-1648\(00\)00488-9](http://dx.doi.org/10.1016/S0043-1648(00)00488-9).
34. Weng W, Biesiekierski A, Lin J, Li Y, Wen C. Impact of rare earth elements on nanohardness and nanowear properties of beta-type Ti-24Nb-38Zr-2Mo alloy for medical applications. *Materialia.* 2020;12:100772. <http://dx.doi.org/10.1016/j.mtla.2020.100772>.